

# 4 Neutrinoless Double Beta Decay with GERDA and LEGEND

Laura Baudis, Roman Hiller, Michael Miloradovic, Rizalina Mingazheva,  
Chloe Ransom

*in collaboration with:* INFN Laboratori Nazionali del Gran Sasso LNGS, Jagellonian University Cracow, Institut für Kern- und Teilchenphysik Technische Universität Dresden, Joint Institute for Nuclear Research Dubna, Institute for Reference Materials and Measurements Geel, Max Planck Institut für Kernphysik Heidelberg, Università di Milano Bicocca e INFN Milano, Institute for Nuclear Research of the Russian Academy of Sciences, Institute for Theoretical and Experimental Physics Moscow, Russian Research Center Kurchatov Institute, Max-Planck-Institut für Physik München, Dipartimento di Fisica dell Università di Padova e INFN, Physikalisches Institut Eberhard Karls Universität Tübingen.

(GERDA and LEGEND Collaborations)

## 4.1 Introduction

Neutrinos are the only known elementary particles that are Majorana fermion candidates, implying that they would be their own antiparticles. The most sensitive and perhaps only practical probe for the Majorana nature of neutrinos is an extremely rare nuclear decay process called neutrinoless double beta decay ( $0\nu\beta\beta$ ), where a nucleus with mass number  $A$  and charge  $Z$  decays by emitting two electrons and changes its charge by two units  $(A,Z)\rightarrow(A,Z+2) + 2e^-$ . The observation of this decay would mean that the lepton number is violated by two units, and would yield information on the neutrino mass scale via the so-called effective neutrino Majorana mass  $\langle m_{\beta\beta} \rangle = |\sum_i U_{ei}^2 m_i|$ , where the sum is over the neutrino mass eigenstates  $m_i$ , and  $U_{ei}$ , the corresponding entries in the lepton mixing matrix, are complex numbers. The related, two-neutrino double beta decay mode ( $2\nu\beta\beta$ ) is allowed in the Standard Model and has been observed in more than 10 nuclei. In this case, the sum energy of the two electrons is a continuum, while for the  $0\nu\beta\beta$ -decay the distinct signature is a peak at the  $Q$ -value, the mass difference between mother and daughter nucleus.

Experiments can observe a certain decay rate in a detector, the half-life of which is inversely proportional to  $\langle m_{\beta\beta} \rangle^2$ :

$$\frac{1}{T_{1/2}^{0\nu}} = \frac{\langle m_{\beta\beta} \rangle^2}{m_e^2} G^{0\nu} |M^{0\nu}|^2, \quad (4.2)$$

assuming that the decay is mediated by the exchange of a light Majorana neutrino, and where  $m_e$  is the mass of the electron, while  $G^{0\nu}$  and  $M^{0\nu}$  are the phase space factor and the nuclear matrix element, respectively. Recent experimental limits on  $T_{1/2}^{0\nu}$  and  $\langle m_{\beta\beta} \rangle$  are of the order  $T_{1/2}^{0\nu} \geq 10^{25}$ - $10^{26}$  y and  $\langle m_{\beta\beta} \rangle \leq 0.06 - 0.4$  eV, using a variety of nuclei and detector technologies.

## 4.2 The GERDA Experiment

The GERDA experiment aims to detect the  $0\nu\beta\beta$  decay of  $^{76}\text{Ge}$ , and is currently acquiring science data in its second phase at the Laboratori Nazionali del Gran Sasso (LNGS). GERDA uses high-purity germanium diodes, enriched in  $^{76}\text{Ge}$ . The diodes, arranged in seven strings, act simultaneously as the detector and source material and are submerged in liquid argon (LAr). A water Cherenkov veto surrounds the LAr cryostat, to reject interactions from cosmic muons. Filled with ultra-pure water, the water tank also provides shielding against external radiation. The LAr cryostat is instrumented as a veto against background events from Compton scatters. It is equipped with photomultiplier tubes and silicon photomultipliers (SiPMs) to detect the scintillation light induced by interactions in the argon, triggered by an event in a germanium detector. The upgraded instrument is described in [1], and the latest results from this second phase of the project can be found in [2, 3]. The next phase, called GERDA-Upgrade is a step towards a 200 kg stage, to be constructed at LNGS by the new collaboration, LEGEND [4], which itself is the precursor of a future, ton-scale  $^{76}\text{Ge}$  experiment. The aimed sensitivities are  $T_{1/2}^{0\nu\beta\beta} > 10^{26}$  y and  $T_{1/2}^{0\nu\beta\beta} > 10^{27}$  y for GERDA-Upgrade and the 200 kg stage, respectively.

- [1] M. Agostini *et al.* [GERDA Collaboration], arXiv:1710.07776 [nucl-ex], accepted in EPJ-C.
- [2] M. Agostini *et al.*, [GERDA Collaboration] Nature **544** (2017) 47-52.
- [3] M. Agostini *et al.* [GERDA Collaboration], Phys. Rev. Lett. **120** (2018) no.13, 132503
- [4] N. Abgrall *et al.* [LEGEND Collaboration], AIP Conf. Proc. **1894** (2017) no.1, 020027, [arXiv:1709.01980]

### 4.3 Search for the $0\nu\beta\beta$ -decay

GERDA has been successfully operated in its second phase starting from December 2015. Over this period, the experiment has achieved the lowest background ever in the region of interest for the neutrinoless double beta decay ( $Q_{\beta\beta} \pm 25$  keV) (see Table 4.1). In consequence, less than one background event for the designed exposure of 100 kg·y [5] is expected. This low-background level has been achieved thanks to enhanced background rejection algorithms, and to the upgrade campaign in the summer 2015, which included the instrumentation of the liquid argon veto, the addition of 30 Broad Energy Germanium (BEGe) detectors (total mass of 20.0 kg) to the enriched coaxial detectors (15.6 kg), and the decreasing background levels of materials surrounding the detectors. The achieved energy resolution at  $Q_{\beta\beta}$  at full width half maximum (FWHM) is about 3 and 4 keV for the BEGe and coaxial detectors, respectively. The latest results include data sets published in [5] and [6]. The summary of the obtained exposure and measured background index (events per keV·kg·y) during the second phase are summarised in the Table 4.1. The analysis includes in addition physics data accumulated during the first phase of the experiment, which makes 23.5 kg·y in total [7]. The efficiency  $\epsilon$  is given by the product of the  $^{76}\text{Ge}$  isotope fraction ( $\sim 87\%$ ), the active volume fraction (85%/89%), the efficiency of  $0\nu\beta\beta$  event reconstruction at full energy in a single detector ( $\sim 92\%$ ), the efficiency of the pulse shape discrimination algorithm (79%-87%) and the liquid argon veto acceptance (98%).

Figure 4.1 shows the overall energy spectrum accumulated for the enriched BEGe detectors prior and after applied cuts for background re-

TABLE 4.1 – Summary of the exposure, resolution (FWHM), efficiency and expected background contribution for two Phase II data sets in GERDA.

| Data set | exp. | resolution | efficiency | background  |
|----------|------|------------|------------|---|
|          | kg·y | keV        |            | $\frac{10^{-3}\text{cts}}{\text{keV}\cdot\text{kg}\cdot\text{y}}$ |
| Coaxial  | 5.0  | 4.0(2)     | 0.53(5)    | $3.5^{+2.1}_{-1.5}$   |
| BEGe     | 18.2 | 2.93(6)    | 0.60(2)    | $1^{+0.6}_{-0.4}$   |

jection. The zoom into the region of interest in Fig. 4.2 shows the data from Phase I, as well as the Phase II data divided into enriched coaxial and BEGe detectors. The analysis range is from 1930 keV to 2190 keV, excluding indicated intervals which correspond to known peaks predicted by the background model.

After all the event selection criteria were applied and the region of interest around the  $Q$ -value of the decay was unblinded, four events were observed for BEGe and coaxial detectors, respectively (as seen in Fig. 4.2) for Phase II data. Since there are no events close to  $Q_{\beta\beta}$  we place a 90% C.L. lower limit of  $T_{1/2}^{0\nu} > 8.0 \times 10^{25}$  y on the decay half-life derived from a frequentist analysis, with a median sensitivity of  $5.8 \times 10^{25}$  y [6].

[5] M. Agostini *et al.*, [GERDA Collaboration] Nature **544** (2017) 47-52.

[6] M. Agostini *et al.* [GERDA Collaboration], Phys. Rev. Lett. **120** (2018) no.13, 132503

[7] M. Agostini *et al.*, Phys. Rev. Lett. **111** (2013) 122503.

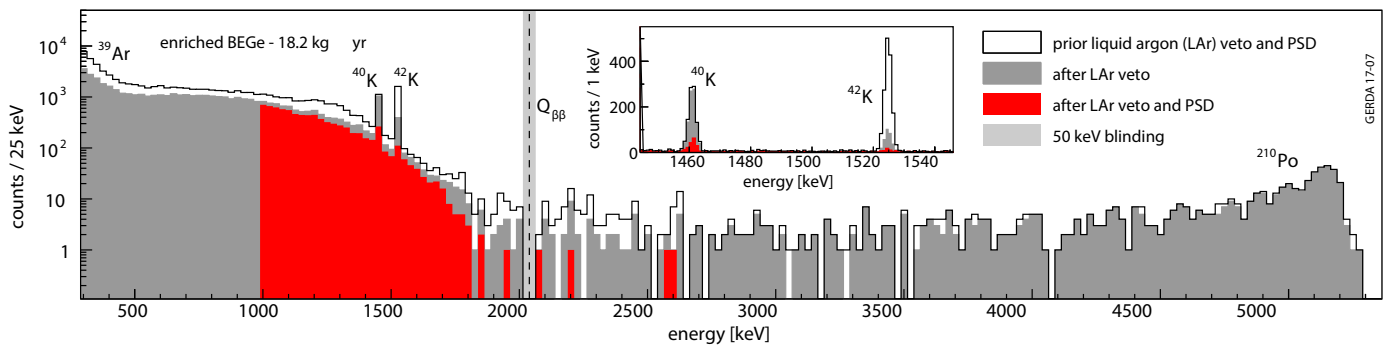


FIG. 4.1 – Energy spectra of Phase II BEGe detectors prior to liquid argon veto and PSD cuts (open histogram), after the LAr veto (dark grey) and after all event selection criteria (red). The inset shows the spectrum in the energy region of the gamma lines from  $^{40}\text{K}$  and  $^{42}\text{K}$ . The blinded region of  $\pm 25$  keV around  $Q_{\beta\beta}$  is indicated with the grey vertical band.

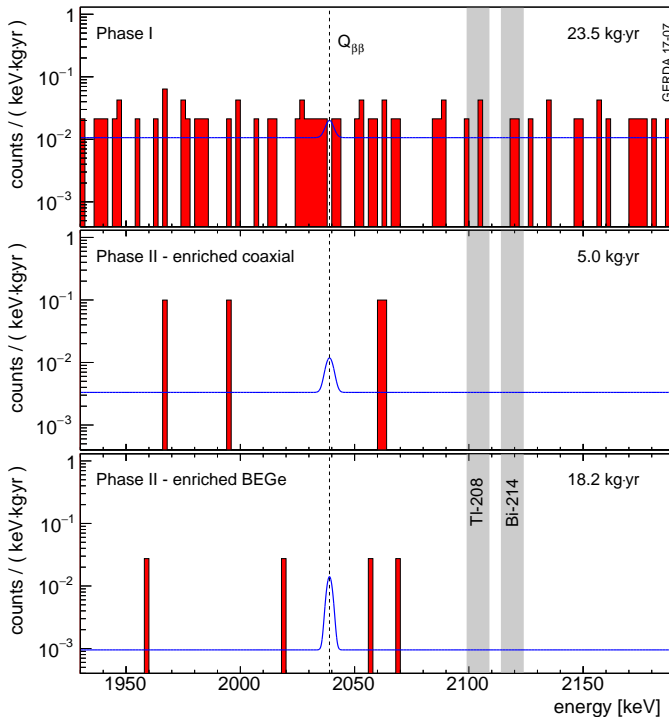


FIG. 4.2 – Energy spectra in the analysis range for Phase I and Phase II coaxial and BEGe detectors, respectively, after all the event selection criteria are applied (red histograms). The grey vertical bands indicate the intervals excluding known gamma lines. A hypothetical  $0\nu\beta\beta$  signal for  $T_{1/2}^{0\nu} = 8.0 \times 10^{25}$  y together with the expected background is also shown (blue lines).

16

#### 4.4 Energy calibration and resolution

Knowledge of the energy scale and resolution of the GERDA detectors is required for all physics analyses. In addition, the energy resolution at the  $Q$ -value of  $0\nu\beta\beta$  decay is a strong prior for the sensitivity. Germanium detectors have excellent resolutions, of about 3–4 keV at FWHM, which improves the sensitivity for all peak searches. The array is calibrated by temporarily exposing the germanium detectors to  $^{228}\text{Th}$  sources on an approximately weekly basis. Our group is jointly responsible for performing the weekly calibrations and for analysing and evaluating the calibration data.

The combined analysis for the energy resolution at  $Q_{\beta\beta}$  is shown in Fig. 4.3. Since the GERDA background level is very low, as explained in section 4.3, there are few gamma lines whose resolution can be used as a cross-check for this analysis. The resolution of the  $^{42}\text{K}$  line at 1525 keV is also shown in Fig. 4.3. For the coaxial detectors, the resolution in physics data is somewhat poorer than expected from calibration data. The reason for this is not yet clear, and investigations are ongoing.

We have studied systematic uncertainties on the energy scale determination, by considering deviations in

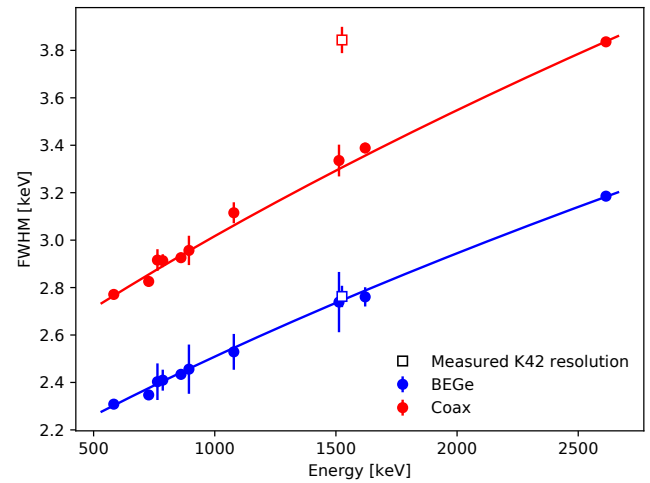


FIG. 4.3 – Combined energy resolution curves for BEGe (blue) and coaxial (red) detectors using data acquired with the  $^{228}\text{Th}$  calibration sources (filled symbols). The estimated resolution based on low-background data using the  $^{42}\text{K}$  line at 1525 keV is also shown for comparison (open symbols). The observed systematic difference for coaxial detectors is currently under investigation.

the observed peak positions of the combined calibration spectra from their literature values. These could be caused by non-linearities present in the energy scale. For the BEGe and coaxial detectors, we estimate an uncertainty in the energy scale at  $Q_{\beta\beta}$  of 0.2–0.3 keV and 0.2–0.4 keV respectively.

The relatively short half-life of  $^{228}\text{Th}$  of 1.9 y requires that the three sources be replaced regularly. We are currently producing the new sources, in collaboration with the company Eckert & Ziegler, Mainz University and the Paul Scherrer Institute, with the deposition of thorium on gold foils foreseen for June this year. The deposition will be followed by the encapsulation and subsequent characterisation of the produced sources, including the determination of their activities and cryogenic tests. The current GERDA sources were also produced and characterised by our group [8], and we will follow a similar recipe for this round of calibration sources.

[8] L. Baudis *et al.*,

Journal of Instrumentation **10**, 12 (2015) P12005.

#### 4.5 Background model and pulse shape simulations

We are part of the background modelling effort in the GERDA collaboration. It is based on Monte Carlo simulations of radioactive isotope decays in the detector materials [9], together with measured radioactivity levels using low-background germanium spectroscopy.

So far, the focus of the collaboration was on the enriched germanium detectors, which are used for the main

physics analysis of the  $0\nu\beta\beta$ -decay channel. Recently, we have started to investigate the natural (non-enriched) germanium detectors (placed on the central detector string in GERDA), with the goal of including these in the overall background model. These detectors, while fewer in number than the enriched diodes (3 diodes, with a total mass of 7.6 kg), have the advantage that the background due to the  $2\nu\beta\beta$ -decay is lower, as  $^{76}\text{Ge}$  is present in natural Ge with an abundance of 7.8%. The energy spectrum thus provides complementary information on some background components. As an example, additional  $^{214}\text{Bi}$  peaks are visible and will provide clues on the source location, which depends on the ratio of observed peak intensities. Our preliminary background model for the natural Ge detectors is shown in Fig. 4.4. No major discrepancies in peaks are visible that allude to other poten-

tial components that could be fit to the data. Some smaller differences have been investigated and excluded as being from additional radioactivity. Several  $^{214}\text{Bi}$  peaks not visible in the enriched coaxial detector spectrum are revealed in a zoom into the background region visible in the lower part of Fig. 4.4. These stem mostly from  $^{214}\text{Bi}$ , while  $^{85}\text{Kr}$  and  $^{39}\text{Ar}$  peaks are visible as well.

Currently, all the background model simulations are limited to the energy deposition inside the germanium detectors and do not include the signal generation in the Ge diodes. The impact of the detector response and signal processing, as well as the pulse shape properties required for pulse shape discrimination (PSD) are thus not accounted for. We have developed tools in order to integrate the Monte Carlo simulations of the background (based on Geant4) into the pulse shape simulation software. The main goal is to perform an end-to-end simulation of GERDA events and to develop a background model after PSD, which can be directly compared with data. To this end, we have first developed an interface that extracts the detector geometries and transforms the Monte Carlo hits into the detector frame based on the geometries. The subsequent field simulations in each detector then use the extracted geometries.

To validate the pulse shape simulation results, we have performed a first comparison between averaged simulated pulses created with hits from simulations of the double escape peak (DEP) of the  $^{208}\text{Tl}$  line with real pulses taken from the DEP in GERDA Phase II calibration data. The result is shown in Fig. 4.5. The simulation agrees well with the data up to a 2% level, where the op-

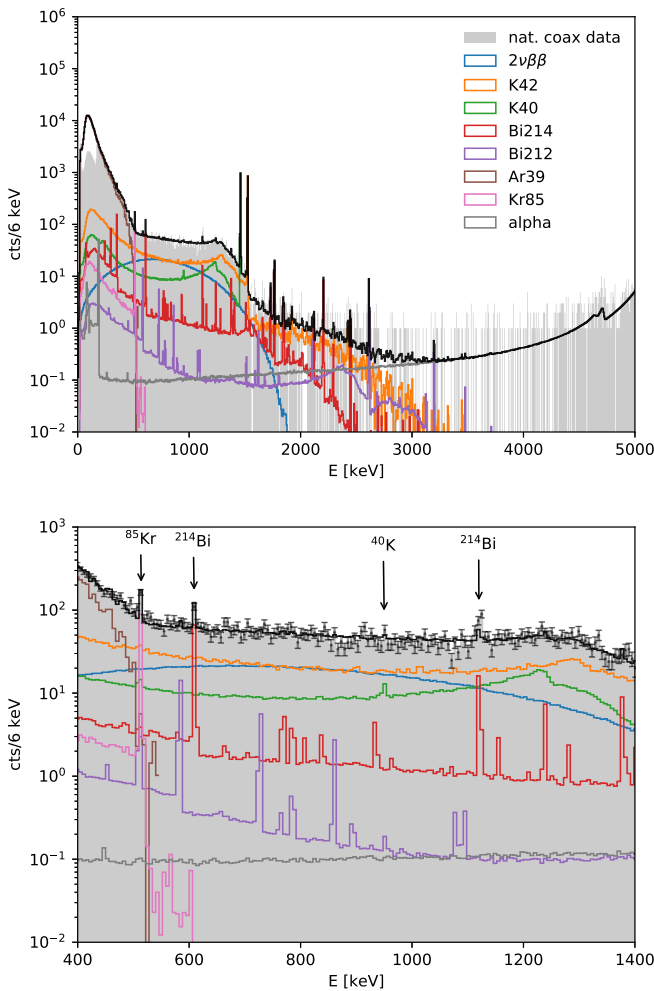


FIG. 4.4 – Preliminary background model fit of Monte Carlo simulations of the most dominant background components to data of the validated dataset of the natural coaxial detectors (grey). Top: Full energy range from 0 to 3000 keV. Bottom: Zoom into range from 400 to 1400 keV revealing peaks which are only visible for natural coaxial detectors.

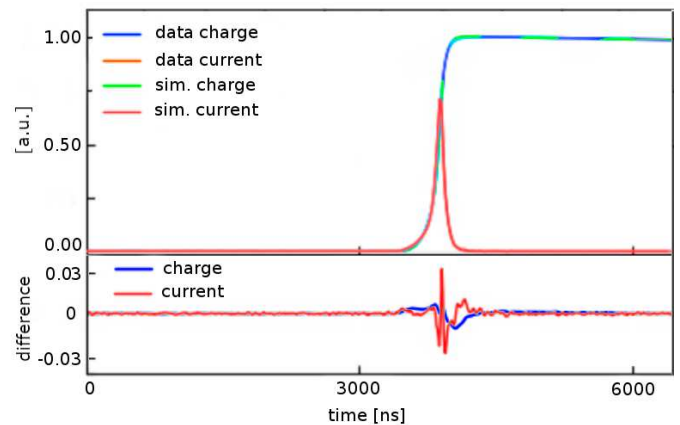


FIG. 4.5 – Averaged waveforms of events in the Double Escape Peak of  $^{208}\text{Tl}$  from pulse shape simulations and recorded data. Top: Average simulated charge and current pulses (green, red) of BEGe detectors from calibration data in comparison to the corresponding average data pulses (blue, orange) from calibration data. Bottom: The difference between simulations to data for charge (blue) and current (red) pulses.

timisation of the simulation parameters is expected to further reduce this in the future. Our next step is to run the simulated pulses through the entire GERDA data production chain, and after validating the calibration spectra, to build a background model which incorporates PSD.

[9] M. Agostini *et al.*, *Eur. Phys. J. C* (2014) **74**: 2764.

#### 4.6 The GERDA Upgrade and LEGEND

Considering the background level and energy resolution achieved by GERDA [10, 11], the projected sensitivity on  $T_{1/2}^{0\nu\beta\beta}$  surpassed  $10^{26}$  y in early 2018 - the first experiment to do so. A major data release is planned for summer 2018, with the unblinding of the new data sets scheduled for May. With its unprecedented low background, GERDA remains in the "background-free" regime, where the sensitivity grows linearly with exposure. Thus, to fully exploit the potential of the experiment, we are upgrading the detector and increase the target mass to achieve a higher final exposure by the end of 2019.

In May 2018, all the detector strings will be extracted from the liquid argon and modified as follows: The three natural germanium detectors with a mass of 7.6 kg, together with the lightest (800 g) enriched coaxial type detector, will be replaced by five newly built, enriched inverted coaxial type detectors [12] with a total mass around 9 kg. With the increased target mass of enriched germanium GERDA will have caught up the lost uptime due to the hardware upgrade within a few months. This will be the first time that this new detector type will be operated long-term in liquid argon, thus providing a vital test for the next-generation experiment LEGEND, which is to employ inverted coaxial detectors on a larger scale.

Apart from installing new detectors, we aim to suppress the background in GERDA even further, by introducing two modifications. The optical fibre shroud around the detector strings will be replaced by a new, denser one to improve the efficiency of the liquid argon veto. We will also replace part of the cables to reduce the radioactivity inside the cryostat. Should GERDA observe a first signal, it will benefit from a lower background level, because the sensitivity for signal detection is more sensitive to background and can still be improved. If no signal will be detected, we will demonstrate that an even lower background index is achievable, which will be a crucial step towards the ambitious background goals of LEGEND.

Finally, smaller repairs and modifications are planned: The amplifiers of three detectors were damaged by power

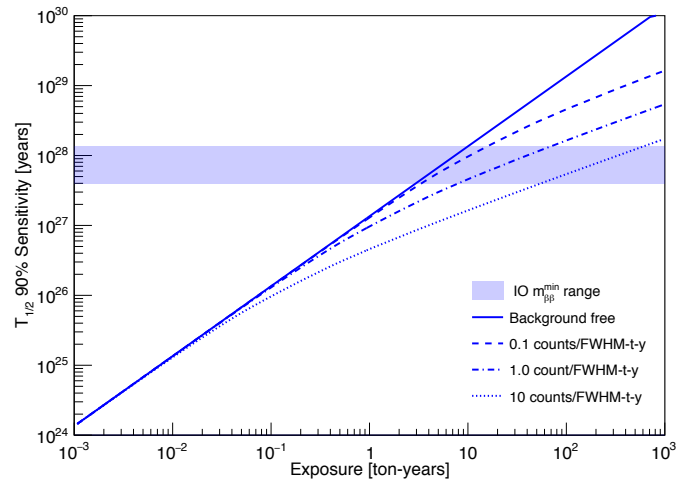


FIG. 4.6 – Sensitivity for a signal discovery in LEGEND, shown as the half-life sensitivity versus exposure. The four curves imply different background scenarios, and the horizontal light blue region shows the effective Majorana neutrino range for the inverted mass ordering scenario.

surges and will be repaired. All amplifiers will be modified to avoid similar damage in the future and reduce their noise. A few detectors with an increased leakage current will be etched for stabilising their performance. The detector holders will be modified to operate all detectors upright to avoid additional leakage current due to particulates accumulating on the groove between the electrodes if it is faced upwards.

Once GERDA Phase II ends in late 2019, the cryostat will be modified for housing the first stage of LEGEND [13], the LEGEND-200 experiment. This experiment will combine enriched germanium detectors from GERDA, the Majorana Demonstrator, as well as newly produced diodes to achieve a target mass of 200 kg. The aim is to operate in background-free mode up to an exposure of 1000 kg·y and thus to increase the sensitivity to the half-life by one order of magnitude (Fig. 4.6). LEGEND will be a first step towards a ton-scale germanium experiment. A ton-scale experiment would probe the inverted neutrino mass ordering scenario.

[10] M. Agostini *et al.*, *Nature* **544** (2017) 47-52.

[11] M. Agostini *et al.*, *Phys. Rev. Lett.* **120** (2018) 132503.

[12] A Domula *et al.*, *Nucl. Instrum. Meth. A* **891** (2018) 106-110.

[13] N. Abgrall *et al.* [LEGEND Collaboration], *AIP Conf. Proc.* **1894** (2017) no.1, 020027, [arXiv:1709.01980]